Renewable Energy, Environment, and Power Quality Journal (REE&PQJ)
ISSN:3020-531X
Volume 26, July 2026

# Grid Resilience under high shares of Non-Synchronous Generation: Insights from the 2025 Iberian Peninsula Blackout

S. Martín-Arroyo[1], M. García-Gracia[1], J.A. Cebollero[1], Á. Llamazares[1] and O. Anaya-Lara[2]

[1] Department of Electrical Engineering
EINA, Zaragoza University
María de Luna 3 – Edificio Torres Quevedo – Campus Río Ebro – 50018 Zaragoza (Spain)
e-mail: smartin@unizar.es, mggracia@unizar.es, joseac@unizar.es, allamaza@unizar.es

[2] Department of Electronic and Electrical Engineering
Faculty of Engineering, University of Strathclyde, Glasgow, UK
Royal College Building, 204 George Street, Glasgow, G1 1XW, UK
e-mail: olimpo.anaya-lara@strath.ac.uk

**Abstract.** This paper investigates grid resilience in power systems with high shares of non-synchronous generation, using the 28 April 2025 Iberian Peninsula disturbance as a real-world case study. The objective is to characterize the dynamic mechanisms governing instability propagation under structurally low-inertia conditions. The study integrates high-resolution measurement analysis, dynamic event reconstruction, and a layered root-cause framework that distinguishes the initiating network disturbance from subsequent amplification processes. Results indicate that fast inter-area oscillations emerged in a context of reduced synchronous generation, leading to elevated rate-of-change-of-frequency (RoCoF) values and accelerated frequency decline. The interaction between grid-following inverter-based resources, RoCoF-sensitive protection schemes, and constrained interconnection capacity contributed to cascading generation and load disconnections. The reduced effective inertia significantly limited the time available for corrective control actions, amplifying system vulnerability. The paper concludes that ensuring resilience in low-inertia grids requires explicit inertia and fast frequency response adequacy criteria, deployment of grid-forming converter capabilities, adaptation of protection settings to high-RoCoF environments, and reinforcement of cross-border support mechanisms. The findings provide a structured analytical basis for the design of stability services in future renewable-dominated power systems.

**Key words.** Power system stability, grid resilience, low-inertia systems, nonsynchronous generation, blackout analysis.

## 1. Introduction

Modern power systems are undergoing a structural transformation driven by decarbonization policies and the large-scale integration of renewable energy sources (RES). As synchronous generation is progressively displaced by inverter-based resources (IBRs), overall system inertia decreases, reducing frequency stability margins and increasing sensitivity to fast disturbances. The implications of inertia reduction for frequency dynamics and system operation have been extensively analyzed in the literature, showing the intensification of rate-of-change-of-frequency (RoCoF) and the reduction of available corrective response time following major imbalances [1], [2].

Beyond the classical swing-equation interpretation of frequency stability, recent studies have explored analytical and simulation-based approaches to quantify the impact of low inertia on frequency nadir, RoCoF thresholds, and stability margins in renewable-dominated systems [3]. In parallel, composite resilience metrics integrating inertia adequacy, disturbance magnitude, and reserve activation time have been proposed to better characterize stability limits in high-RES grids [4]. The provision of synthetic inertia and fast frequency response through power-electronic converters has also been widely investigated as a mitigation strategy [5].

From an operational and regulatory perspective, European technical reports have emphasized the growing importance of grid-forming capabilities, improved modeling of IBRs, and enhanced coordination between protection and control layers in systems with high penetration of power-electronic-interfaced generation [6], [7].

The large-scale disturbance that affected the Iberian Peninsula on 28 April 2025 provides a relevant real-world validation context for these theoretical considerations. According to the updated technical reconstruction published by ENTSO-E, the event involved fast dynamic interactions under reduced synchronous generation conditions, leading to cascading disconnections and widespread outages [8]. Independent technical assessments have further highlighted structural planning and stability-service adequacy issues in high-renewable operating scenarios [9].

This paper applies an aggregated dynamic reconstruction approach and a structured root-cause framework to the 2025 Iberian disturbance, linking empirical observations with resilience metrics suitable for future renewable-dominated power systems.

## 2. Methodological Framework

This study adopts a dual-layer methodological approach combining empirical disturbance reconstruction with simplified dynamic modeling. The objective is to bridge real-event analysis with theoretical frequency dynamics in low-inertia systems.

First, the 28 April 2025 Iberian disturbance is analyzed using publicly available technical reports and documented system behavior [8], [9]. The reconstruction focuses on identifying the sequence of events, the operating conditions prior to the disturbance, and the mechanisms that contributed to instability propagation, including inertia scarcity and protection interactions.

Second, a simplified aggregated dynamic model based on the classical swing equation is implemented in MATLAB. This representation is widely used to characterize the short-term response of low-inertia systems [1], [2]. The purpose of this model is not to replicate the Iberian system in detail, but to quantify the sensitivity of frequency dynamics to inertia reduction under controlled conditions, consistent with recent analytical investigations on renewable-dominated grids [3].

By applying an equivalent step disturbance representing sudden generation loss, the model enables comparison of RoCoF, frequency nadir, and critical response time for different inertia constants. This complementary approach allows validation of qualitative observations derived from the real event and quantitative assessment of inertia-scarcity effects.

## 3. Aggregated Dynamic Model

To quantify the impact of inertia reduction on frequency dynamics, a simplified aggregated system model was implemented in MATLAB. The model represents the equivalent electromechanical behavior of a synchronous area using a single-machine approximation governed by the classical swing equation.

*A. Frequency Dynamic Representation*

The short-term frequency evolution following a disturbance is described by (1).

$$\frac{2H}{f_0}\frac{df}{dt} = \Delta P - D\Delta f \qquad (1)$$

where $H$ is the inertia constant (s), $f$ and $f_0$ are the instantaneous and nominal frequencies (Hz), $t$ is time (s), $\Delta P$ is the power imbalance (pu), $D$ is the damping coefficient (pu/Hz), and $df/dt$ is the RoCoF (Hz/s).

This aggregated formulation is widely adopted for assessing inertia-dependent frequency behavior in low-inertia systems [1], [2].

For simulation purposes, the nominal frequency was set to 50 Hz, with a damping coefficient of $D$ = 0.05 pu/Hz. The disturbance was modeled as a $\Delta P = -0.15$ pu step, representing a 15% sudden generation loss applied to the system base power. Different inertia values were considered to evaluate the sensitivity of frequency dynamics to inertia reduction. The simulation horizon was limited to 10 s to capture the inertial response and the early post-fault dynamics.

*B. Disturbance Modeling*

A step disturbance representing sudden generation loss was applied to the model. The disturbance magnitude was defined as a percentage of total system base power, ensuring scalability and avoiding reliance on confidential operational data. The 10-second simulation window captures the fast-inertial response and the onset of primary frequency control.

*C. Inertia Scenarios*

Three representative inertia constants were considered:

- $H$ = 6 s (high inertia)
- $H$ = 4 s (medium inertia)
- $H$ = 2 s (low inertia)

These values reflect typical ranges reported in European interconnected systems under varying renewable penetration levels [2], [3].

*D. Performance Indicators*

The following indicators are extracted from the simulations:

- Initial RoCoF ($df/dt$ at $t = 0^+$).
- Frequency nadir (due to the simplified first-order nature of the aggregated dynamic model, which excludes governor and secondary control dynamics, the frequency trajectory exhibits a continuous exponential decay toward a new steady-state operating point. Therefore, the term *nadir* is interpreted here as the quasi-steady-state frequency reached within the evaluated 10-second inertial window, representing the point where the rate of change of frequency approaches zero).
- Time to reach critical frequency thresholds (49.0 Hz, 48.8 Hz).
- Recovery gradient.

These metrics support comparison between inertia levels and complement the empirical observations from the 2025 disturbance.

The proposed model does not attempt to reproduce the exact topology or operational state of the Iberian system, but rather to illustrate dynamic behaviors compatible with publicly reported characteristics of the disturbance. Its purpose is to provide a simplified analytical framework for evaluating how inertia scarcity may amplify frequency excursions and reduce the time available for corrective actions in renewable-dominated power systems.

## 4. Results and Discussion

The aggregated dynamic model provides a quantitative assessment of how inertia reduction affects short-term frequency stability following a sudden generation loss. Figure 1 illustrates the simulated frequency trajectories for the three inertia scenarios, showing a visibly faster frequency decline as inertia decreases.

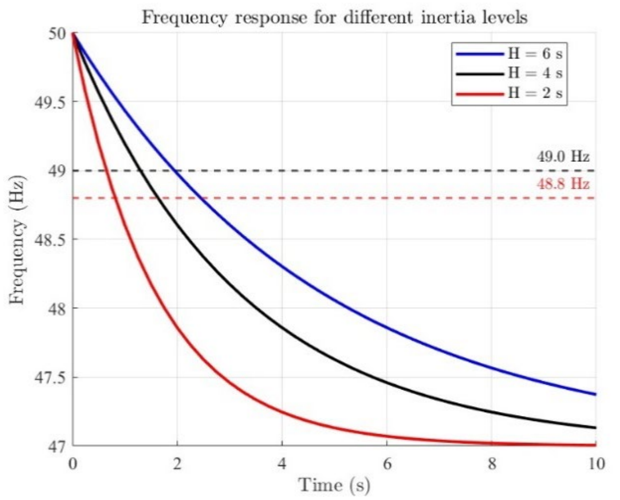

Fig.1. Simulated frequency trajectories for different inertia levels ($H$ = 6 s, $H$ = 4 s, $H$ = 2 s).

The qualitative differences observed in the trajectories are complemented by the numerical key performance indicators summarized in Table I, which quantify RoCoF, nadir depth, and the time required to reach critical frequency thresholds.

Table I. - Frequency stability indicators for different inertia levels

| H (s) | RoCoF (Hz/s) | Nadir (Hz) | Time to Nadir (s) | Time to 49.0 Hz (s) | Time to 48.8 Hz (s) |
|---|---|---|---|---|---|
| 6 | -0.625 | 47.374 | 10.00 | 1.95 | 2.51 |
| 4 | -0.938 | 47.132 | 10.00 | 1.33 | 1.67 |
| 2 | -1.875 | 47.000 | 6.82 | 0.67 | 0.84 |

*A. RoCoF Sensitivity to Inertia*

The simulation results show a clear inverse relationship between system inertia and the initial rate of change of frequency (RoCoF). For the same disturbance magnitude ($\Delta P$ = -0.15 pu), the initial RoCoF values are -0.625 Hz/s ($H$ = 6 s), -0.938 Hz/s ($H$ = 4 s) and -1.875 Hz/s ($H$ = 2 s). This behavior is consistent with the analytical proportionality between RoCoF and $1/H$, confirming that low-inertia operation leads to significantly faster frequency decline. The high RoCoF observed in the $H$ = 2 s case is comparable to values reported during the 28 April 2025 Iberian disturbance [8].

*B. Frequency Nadir and Depth of Frequency Excursion*

The frequency nadir becomes progressively deeper as inertia decreases, dropping from 47.374 Hz ($H$ = 6 s) to 47.132 Hz ($H$ = 4 s) and 47.000 Hz ($H$ = 2 s). The time required to reach this practical stabilization depends heavily on the system inertia, with the low-inertia scenario ($H$ = 2 s) flattening much faster than the higher inertia cases. Specifically, the numerical metrics show that the lowest inertia case stabilizes well before the end of the simulation window, whereas the higher inertia trajectories ($H$ = 4 s and $H$ = 6 s) decay at a slower rate, reaching the 10-second simulation window boundary before full stabilization due to the first-order nature of the model. Lower inertia results in a more pronounced frequency excursion, reducing the available stability margin and increasing the likelihood of under-frequency load shedding or inverter tripping before any primary control can effectively deploy.

*C. Time to Reach Critical Frequency Thresholds*

A key resilience indicator is the time available for corrective actions before the system crosses critical frequency thresholds. The model shows a strong dependence on inertia: the system reaches 49.0 Hz in 1.95 s ($H$ = 6 s), 1.33 s ($H$ = 4 s) and only 0.67 s ($H$ = 2 s). A similar trend is observed for the 48.8 Hz threshold, with crossing times of 2.51 s, 1.67 s, and 0.84 s, respectively. These results highlight a compression of the stability time window as inertia decreases, leaving insufficient time for primary frequency response or emergency control actions in low-inertia conditions.

*D. Implications for Low-Inertia System Operation*

The simulation confirms that inertia scarcity fundamentally alters short-term frequency behavior by increasing RoCoF, deepening the frequency nadir, and reducing the time available for corrective actions. These effects collectively amplify system vulnerability during large disturbances. The correspondence between the simulated trends and the empirical observations from the 2025 Iberian disturbance supports the validity of the aggregated model as a tool for resilience assessment in renewable-dominated power systems.

## 5. Implications for System Operation and Planning

The simulation results highlight several structural vulnerabilities that emerge when power systems operate with reduced synchronous inertia. These vulnerabilities have direct implications for real-time operation, protection coordination, and long-term system planning in renewable-dominated grids.

*A. Inertia Adequacy and Frequency Stability Margins*

The strong dependence of RoCoF and frequency nadir on inertia demonstrates that inertia adequacy must be treated as a fundamental operational constraint. In the low-inertia scenario ($H$ = 2 s), the system reaches 49.0 Hz in less than one second, leaving insufficient time for primary frequency response to counteract the disturbance. This behavior is consistent with the inertia-dependent stability margins reported in ENTSO-E studies [10], [11]. System operators will require explicit inertia requirements or real-time inertia monitoring to ensure that frequency stability margins remain within acceptable limits.

*B. Need for Fast Frequency Response from Inverter-Based Resources*

The rapid frequency decline observed in the low-inertia case underscores the importance of fast frequency response (FFR) capabilities. Grid-following inverter-based resources, which currently dominate renewable generation portfolios, do not inherently contribute to inertial response and may disconnect under high RoCoF conditions. This aligns with ENTSO-E's recommendations on the deployment of grid-forming controls and synthetic inertia [12], [13], and with recent work demonstrating the need for RoCoF-compliant inverter behavior in low-inertia systems [14]. These technologies will be essential to compensate for the reduced mechanical inertia of the system.

As synchronous inertia declines, frequency support must be delivered on faster timescales (from sub-second to a few seconds) via FFR and/or grid-forming controls, so that frequency is arrested before protection thresholds are reached—thereby reducing the system's reliance on synchronous inertia for acceptable frequency performance [2], [15], [16]. In this context, converter-interfaced resources are expected to provide both "virtual-inertia-like" behavior and rapid active-power injection that shape frequency dynamics, complementing and, in some cases, partially displacing the role traditionally played by synchronous machines [15]–[17].

Inertia effectively "buys time": with less inertia, the same power imbalance produces a larger RoCoF and a shorter window for corrective action [2]. Conventional primary frequency response based on governor action is often too slow to adequately limit RoCoF and protect the frequency nadir under very low-inertia conditions; this motivates the deployment of FFR from storage and inverter-based generation, together with grid-forming control strategies that emulate key synchronous-machine characteristics [2], [16], [18]. However, FFR is not "free inertia": its effectiveness depends on measurement and control delays, available headroom and energy, and coordination with other controls and protection—requirements that are increasingly codified in grid codes and interoperability standards for inverter-based resources, such as IEEE Std 2800-2022 [18], [19].

### *C. Protection Coordination Under High-RoCoF Conditions*

The simulation confirms that low inertia leads to RoCoF values that exceed typical protection thresholds. This is consistent with the 2025 Iberian disturbance [8] and with ENTSO-E's findings on the need to revise RoCoF withstand capabilities [20]. Similar concerns have been highlighted in the literature, where RoCoF-based protections have been shown to trigger unintended islanding or disconnection events under fast frequency excursions [14], [21]. As renewable penetration increases, protection settings must be adapted to avoid unnecessary tripping during fast but recoverable frequency excursions.

### *D. Cross-Border Support and System-Wide Coordination*

The reduced time to reach critical frequency thresholds highlights the importance of rapid cross-border support. Inertia scarcity limits the time available for HVDC interconnectors and neighboring systems to provide stabilizing power injections. This observation is aligned with ENTSO-E's System Needs Study [13] and the lessons learned from the 2025 Iberian event [8]. Enhancing interconnection capacity, reducing response delays, and coordinating emergency controls across synchronous areas will be essential to maintain resilience in future operating conditions.

### *E. Planning for Renewable-Dominated Grids*

From a planning perspective, the results emphasize that future grid designs must incorporate stability services as integral components of renewable integration strategies. This includes ensuring sufficient synchronous or synthetic inertia, procuring fast frequency response as a standard ancillary service, reinforcing transmission corridors, and modeling inverter-based resources with adequate dynamic detail. These needs are consistent with ENTSO-E's Future System Architecture framework [22] and with recent analyses showing that RoCoF-sensitive protections and islanding detection schemes must be redesigned for high-RES systems [14], [21]. The aggregated model used in this study, while simplified, provides a transparent framework for assessing how different inertia levels affect system resilience.

## 6. Conclusions

This work has analyzed the influence of inertia scarcity on short-term frequency stability using a simplified aggregated dynamic model. Despite its reduced complexity, the model successfully reproduces the fundamental mechanisms governing frequency evolution after a sudden generation loss, and the obtained results are consistent with both ENTSO-E technical assessments and recent findings in the literature.

The simulations show that decreasing system inertia leads to a substantially higher initial RoCoF, a deeper frequency nadir, and a significant reduction in the time available for corrective actions. In the low-inertia scenario ($H$ = 2 s), the system reaches 49.0 Hz in less than one second, illustrating the structural vulnerability of renewable-dominated systems operating with limited synchronous inertia. This behavior mirrors the dynamics observed during the 2025 Iberian Peninsula disturbance, where high RoCoF values and rapid frequency decline contributed to widespread disconnections.

The results also highlight the need to adapt protection schemes to the new operating conditions. RoCoF-based protections, widely deployed in distributed generation and microgrids, have been shown to be sensitive to fast frequency excursions and may trigger unintended islanding or disconnection events if not properly coordinated [14], [20]. Ensuring compliance with ENTSO-E recommendations and relevant grid codes will be essential to avoid unnecessary tripping during transient but recoverable disturbances.

From an operational perspective, the findings reinforce the importance of maintaining minimum inertia levels or deploying synthetic inertia and fast frequency response (FFR) capabilities to stabilize the system during the first seconds after a disturbance. From a planning perspective, the results support the growing consensus that future power systems must integrate stability services—such as grid-forming control, inertia emulation, and enhanced protection coordination—as core elements of renewable integration strategies.

Overall, the aggregated model provides a transparent and effective analytical tool for illustrating the relationship between inertia and frequency resilience. Its alignment with real-world events and established technical literature confirms its value for supporting system operation, protection design, and long-term planning in high-RES power systems.

## Acknowledgements

The authors express their gratitude to the Research Group on Renewable Energy Integration (GENER) at the University of Zaragoza, accredited and funded by the Government of Aragón (code T30_23R), for their support during the development of this work.

The authors also acknowledge the Department of Electronic and Electrical Engineering at the University of Strathclyde (Glasgow, UK) for hosting a research stay that contributed to this study, and they extend their sincere appreciation to Professor Olimpo Anaya-Lara for his guidance and valuable insights.

## References

[1] P. Tielens and D. Van Hertem, “The relevance of inertia in power systems,” *IEEE Transactions on Power Systems*, vol. 32, no. 3, pp. 2147–2155, 2017.

[2] F. Milano, F. Dörfler, G. Hug, D. J. Hill, and G. Verbič, “Foundations and challenges of low-inertia systems,” *IEEE Transactions on Power Systems*, vol. 35, no. 1, pp. 318–328, 2020.

[3] J. Morren, S. W. H. de Haan, W. L. Kling and J. A. Ferreira, “Wind turbines emulating inertia and supporting primary frequency control,” *IEEE Transactions on Power Systems*, vol. 21, no. 1, pp. 433–434, 2006.

[4] J. Silva, P. Gómez, A. Torres and M. Ruiz, “Stability and Resilience Metrics for Low-Inertia Power Systems,” *Renewable Energy and Power Quality Journal*, no. 20, Paper 307, 2020.

[5] U. Tamrakar, D. Shrestha, B. Bhattarai, A. M. Gole and R. Tonkoski, “Virtual inertia: Current trends and future directions,” *Applied Energy*, vol. 227, pp. 165–174, 2018.

[6] ENTSO-E, *High Penetration of Power Electronic Interfaced Power Sources and the Potential Contribution of Grid Forming Converters*, Brussels, Belgium, 2020.

[7] CIGRÉ Working Group C4.47, *Power System Technical Performance Issues Related to High Penetration of Inverter-Based Resources*, Technical Brochure, 2023.

[8] ENTSO-E, *Updated Technical Report on the Iberian Disturbance of April 2025*, Brussels, Belgium, 2025.

[9] Fundación para el Fomento de la Innovación Industrial (FFII), *Causa y soluciones del apagón*, Technical Assessment, 2025.

[10] ENTSO-E, *Frequency Stability Evaluation Criteria for the Synchronous Zone of Continental Europe*, Technical Report, 2020.

[11] ENTSO-E, *Inertia Monitoring and Dynamic Study Model for Continental Europe*, Technical Report, 2021.

[12] ENTSO-E, *High Penetration of Power Electronic Interfaced Power Sources and the Potential Contribution of Grid Forming Technology*, Technical Report, 2022.

[13] ENTSO-E, *System Needs Study*, Technical Report, 2023.

[14] D. Cañete, S. Martín-Arroyo, M. García-Gracia, Á. Llamazares and I. Sáez, “An Anti-islanding protection based on RoCoF compliant with ENTSO-E and IEC 62116,” *Renewable Energy and Power Quality Journal*, vol. 20, pp. 348–352, September 2022.

[15] Y. Gu and T. C. Green, “Power System Stability With a High Penetration of Inverter-Based Resources,” Proc. IEEE, vol. 111, no. 7, pp. 832–853, Jul. 2023, doi: 10.1109/JPROC.2022.3179826.

[16] B. K. Poolla, D. Gross, and F. Dörfler, “Placement and Implementation of Grid-Forming and Grid-Following Virtual Inertia and Fast Frequency Response,” IEEE Trans. Power Syst., vol. 34, no. 4, pp. 3035–3046, 2019, doi: 10.1109/TPWRS.2019.2892290.

[17] X. Lyu and D. Groß, “Grid-Forming Fast Frequency Response for PMSG-Based Wind Turbines,” IEEE Trans. Sustainable Energy, vol. 15, no. 1, pp. 23–38, 2023, doi: 10.1109/TSTE.2023.3263858.

[18] L. Meng et al., “Fast Frequency Response From Energy Storage Systems—A Review of Grid Standards, Projects and Technical Issues,” IEEE Trans. Smart Grid, vol. 11, no. 2, pp. 1566–1581, 2020.

[19] IEEE Std 2800™-2022, IEEE Standard for Interconnection and Interoperability of Inverter-Based Resources (IBRs) Associated with Transmission Electric Power Systems, 2022.

[20] ENTSO-E, *Rate of Change of Frequency (RoCoF) Withstand Capability and Protection Coordination*, Technical Report, 2018.

[21] J.A. Cebollero, D. Cañete, S. Martín-Arroyo, M. García-Gracia and H. Leite, “A Survey of Islanding Detection Methods for Microgrids and Assessment of Non-Detection Zones in Comparison with Grid Codes,” Energies 2022, 15, 460.

[22] ENTSO-E, *Future System Architecture*, Technical Report, 2021.